International Journal of Biometeorology (2018) 62:1645–1655
https://doi.org/10.1007/s00484-018-1564-9

ORIGINAL PAPER

Later springs green-up faster: the relation between onset and completion of green-up in deciduous forests of North America

Stephen Klosterman[1] · Koen Hufkens[1,2,3] · Andrew D. Richardson[1,4,5]

Received: 3 January 2018 / Revised: 15 April 2018 / Accepted: 16 May 2018 / Published online: 31 May 2018

Abstract

In deciduous forests, spring leaf phenology controls the onset of numerous ecosystem functions. While most studies have focused on a single annual spring event, such as budburst, ecosystem functions like photosynthesis and transpiration increase gradually after budburst, as leaves grow to their mature size. Here, we examine the "velocity of green-up," or duration between budburst and leaf maturity, in deciduous forest ecosystems of eastern North America. We use a diverse data set that includes 301 site-years of phenocam data across a range of sites, as well as 22 years of direct ground observations of individual trees and 3 years of fine-scale high-frequency aerial photography, both from Harvard Forest. We find a significant association between later start of spring and faster green-up: -0.47 ± 0.04 (slope ± 1 SE) days change in length of green-up for every day later start of spring within phenocam sites, -0.31 ± 0.06 days/day for trees under direct observation, and -1.61 ± 0.08 days/day spatially across fine-scale landscape units. To explore the climatic drivers of spring leaf development, we fit degree-day models to the observational data from Harvard Forest. We find that the default phenology parameters of the ecosystem model PnET make biased predictions of leaf initiation (39 days early) and maturity (13 days late) for red oak, while the optimized model has biases of 1 day or less. Springtime productivity predictions using optimized parameters are closer to results driven by observational data (within 1%) than those of the default parameterization (17% difference). Our study advances empirical understanding of the link between early and late spring phenophases and demonstrates that accurately modeling these transitions is important for simulating seasonal variation in ecosystem productivity.

Keywords Phenology · Green-up · Forest productivity · Ecosystem model · North America

Introduction

The timing of leaf unfolding determines seasonal shifts in a range of ecosystem processes, from functions such as photosynthesis and transpiration (Fitzjarrald and Acevedo 2001; Peñuelas et al. 2009; Richardson et al. 2013), to trophic interactions associated with forage availability (Pettorelli et al. 2007; Plard et al. 2014). Changes in the annual arrival of spring phenology events of deciduous trees have accompanied global temperature change, as these events typically arrive earlier when temperatures are higher (Schwartz et al. 2006; Menzel et al. 2006; Piao et al. 2007). Combined with a projected delay of the end of the growing season in a warmer climate found in many tree species (Dragoni et al. 2011; Archetti et al. 2013) (although not all; see Vitasse et al. (2009)), earlier spring-time canopy development creates the potential for greater annual net primary production. This raises the possibility that as

Electronic supplementary material The online version of this article (https://doi.org/10.1007/s00484-018-1564-9) contains supplementary material, which is available to authorized users.

✉ Stephen Klosterman
steve.klosterman@gmail.com

[1] Department of Organismic and Evolutionary Biology, Harvard University, 26 Oxford St, Cambridge, MA 02138, USA

[2] UMR 1391 ISPA – Interactions Sol Plante Atmosphère, INRA, 71 Avenue Edouard Bourlaux, 33140 Villenave D'Ornon, France

[3] Faculty of Bioscience Engineering, Ghent University, Coupure Links 653, 9000 Ghent, Belgium

[4] School of Informatics, Computing, and Cyber Systems, Northern Arizona University, PO Box 5693, Flagstaff, AZ 86011, USA

[5] Center for Ecosystem Science and Society, Northern Arizona University, P.O. Box 5620, Flagstaff, AZ 86011, USA

temperatures rise, forests may sequester increasing amounts of atmospheric carbon dioxide (Keenan et al. 2014; Duveneck and Thompson 2017), to the extent that the residence time of carbon in trees is not reduced (Körner 2017), or gains in photosynthesis are not offset by increases in respiration (Piao et al. 2008). Therefore, an understanding of how spring time leaf development responds to temperature is crucial to understanding forest ecosystem function in a changing climate.

Most studies of the relation of climatic variability to springtime leaf development in forests focus on one annual event, usually defined as budburst or first leaf (Cannell and Smith 1983; Hunter and Lechowicz 1992; Chuine 2000; Schwartz et al. 2006). While budburst marks a key point in the growing season, at which foliar photosynthesis and transpiration begin, the magnitude of ecosystem carbon and water fluxes exhibit a steady increase over several weeks as leaves grow to their mature size (Goulden et al. 1996). Surprisingly, comparatively few studies have examined interannual and spatial variability of the "velocity of green-up," or duration of the period from initial appearance of leaves to their maturity.

Similar to the timing of budburst, the velocity of green-up is thought to be under temperature control. The use of accumulated temperatures as a model for the progression of leaf expansion was established in the literature from studies making detailed leaf-scale measurements: degree-days were found to explain increases in leaf width and length during growth of cereal crops (Gallagher 1979) as well as development of sunflower leaves (Granier and Tardieu 1998). At the plant-to-canopy scale, a study using long term phenology observations from two forest sites in New England found that a sigmoid model describing the trajectory of springtime canopy development could be improved by using degree-day sums as parameters in the sigmoid equation (Richardson et al. 2006). A later landscape-scale remote sensing study in the Southern Appalachian forest of North Carolina explored the effect of topographical factors on green-up rates, finding correlations of green-up duration with aspect and elevation, presumably due to differences in radiation load (Hwang et al. 2011). Recently, Yu et al. (2016) found that accumulated temperature, measured by growing degree-days (GDD), could be used along with day length to predict the progression of 24 spring phenology stages for several species under observation at a study site in Wisconsin. However, Donnelly et al. (2017) characterized the effect of accumulated temperature on the start and duration of the spring season for a wider range of tree species at another site in Wisconsin and found that accumulated GDD above a base temperature of 0 °C, starting on January 1, may not be an accurate predictor of either the timing of spring onset or the duration of leaf expansion.

Examining the relationship between the beginning of canopy development and the velocity of leaf expansion, Donnelly et al. (2017) further observed that an early start to preliminary spring transitions did not imply a longer or shorter duration of subsequent phenophases. However, somewhat different conclusions were reached in a study on the phenology of woody and herbaceous plant species in Greenland using phenocams (Westergaard-Nielsen et al. 2017), which found that a later start of green-up was associated with a shorter duration of green-up. A similar observation was made between two contrasting springs, one with a later, faster green-up than the other, in a deciduous forest in New England (Richardson et al. 2009). Therefore, while these three studies concerned different plant species in different growing conditions, together they indicate that if any relation between the start and length of green-up is observed, it is that a later start tends to have a faster green-up.

These recent in situ studies built on the widespread practice of using growing degree-days to model the timing of discrete phenological events such as budburst (Cannell and Smith 1983; Hunter and Lechowicz 1992; Chuine 2000), which had subsequently been extended to include later spring transitions of leaf growth (Richardson et al. 2006; Yu et al. 2016; Donnelly et al. 2017). The degree-day approach for leaf expansion was also adopted to describe forest canopy development in a study of biosphere/atmosphere exchange of carbon dioxide in forest ecosystems, using different critical sums to mark leaf growth initiation and completion (Goulden et al. 1996). This phenology sub-model, with two critical sums of growing degree days defining the endpoints of leaf expansion, became part of the ecosystem model PnET (Aber et al. 1996). While the parameterization of this sub-model has not been evaluated against observational data, it has however been shown that errors in modeling the start of the growing season are a major source of uncertainty in even the most sophisticated terrestrial biosphere models (Richardson et al. 2012).

In the present study, we investigate the relationship between the start and length of green-up using several modes of observation. We examine interannual variation in the timing of these phenophases using canopy-scale data from tower-mounted phenocams (Sonnentag et al. 2012) as well as direct in-situ observations of trees (Richardson and O'Keefe 2009), and spatial variation using fine-scale landscape units observed by aerial drone photography (Klosterman and Richardson 2017a; Klosterman et al. 2018). This enables us to examine the link between spring phenophases using a more geographically extensive, longer, and more methodologically diverse set of observations than has been done previously. We then fit models of budburst and leaf maturity to the visual observation record, using Monte Carlo optimization to estimate the starting date, base temperature, and critical sums of degree-days associated with springtime phenological events. Finally, we use a fitted phenology sub-model to predict ecosystem productivity with the PnET model. We compare fitted model results to results from the default PnET phenology model to determine the effect of increased accuracy in phenology modeling on predictions of ecosystem function.

Methods

Phenocams

We used publicly available phenocam data from 301 site-years across 51 sites located in North America (2 to 16 years per site, sites displayed in Fig. 1 and listed in Table S1) to examine the relation between start and length of green-up at multiple locations (Richardson et al. 2018).

Phenocam sites were spread throughout diverse climate zones; mean annual temperatures at the sites had a minimum of 0.4 °C, a maximum of 21 °C, a mean of 9.4 °C, and a standard deviation of 4.3 °C. Sites were located in ecosystems with deciduous trees and captured repeat digital photography at least once per day. The number of trees in phenocam fields of view varied widely across study sites, from approximately 5 trees up to over 100 trees. Phenocam images included primarily broadleaf deciduous trees common to the temperate zone of eastern North America, except for two sites of mixed-deciduous evergreen forest where evergreens dominated the camera field of view ("harvardbarn" and "groundhog"). For all sites, however, the region of interest (ROI) within the field of view, used to generate results for this study, was composed of deciduous canopy. Camera fields of view were focused on forests except for one camera in an urban public park ("bostoncommon"). Green chromatic coordinate (G_{CC}) was calculated from the ROIs within the images (Sonnentag et al. 2012). G_{CC} is a measure of the pixel brightness of the green channel of digital imagery relative to the total image brightness (sum of brightness over all channels):

$$G_{CC} = G/(R + G + B) \quad (1)$$

where R, G, and B are the average digital numbers, across the ROI, for the red, green, and blue channels, respectively. Phenophase transition dates, representing the beginning and end of green-up, were calculated using a procedure described in Richardson et al. (2018). Briefly, start of green-up was calculated using a 10% threshold ("transition_10") of amplitude in rising springtime greenness, while end of green-up was calculated using a 90% threshold ("transition_90"), and the length of green-up was the duration between these two events. We calculated dates from the daily (i.e., "1-day") G_{CC} time series. To examine the relation between start and duration of green-up across sites, we calculated interannual anomalies from the multi-year means at each site and performed a linear regression on the combined data set of 301 site-years.

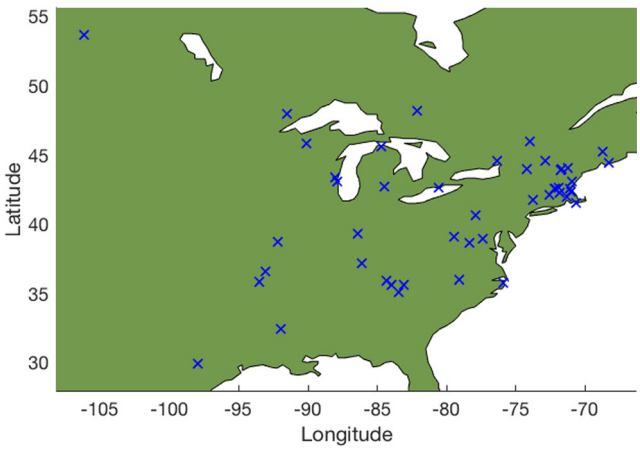

Fig. 1 The 51 phenocam sites, located primarily throughout eastern North America

In situ observations

We used the long-term record of phenology observations from Harvard Forest, which has been widely used in phenology studies, to characterize the timing of leaf development at the individual tree scale (Richardson and O'Keefe 2009; Migliavacca et al. 2012; Jeong et al. 2012; O'Keefe 2015). Start of green-up was characterized as "budburst" (BB), the date when individual trees had recognizable leaves emerging from 50% of the buds, while end of green-up was characterized as "75% leaf size" (L75), the date when 75% of the leaves on an individual reached 75% of their final size. Two to five marked individuals of each species were observed on each date, and we calculated the species-averaged BB and L75 dates for 1993–2004 for the species, *Acer rubrum* (red maple), *Acer saccharum* (sugar maple), *Betula alleghaniensis* (yellow birch), *Fraxinus americana* (white ash), *Quercus alba* (white oak), and *Quercus rubra* (red oak). These are the overstory tree species which have the longest records in the Harvard Forest phenology data set (22 years). We calculated the length of green-up as the period of time from BB to L75.

Aerial drone imagery

We used methods described in an earlier study (Klosterman et al. 2018) to obtain and process aerial photography at Harvard Forest in the vicinity of the EMS tower (42.5377° N, 72.1715° W), over an area of 1.4 ha. We used 3 years of data (2013–2015) in this study. Briefly, we used a drone (3DR ArduCopter Quad-C Frame, 3D Robotics, Berkeley, CA) equipped with a Canon Powershot A3300 camera (35 mm film equivalent focal length 28 mm, approx. 16 million pixels). We took pictures of a gray reference square (ColorChecker classic, X-rite, Grand Rapids, MI) before each flight to ensure data quality (Klosterman and Richardson 2017a; Klosterman et al. 2018). Flight frequency was roughly every 5 days during spring leaf out, every 4 weeks during summer, and every week during autumn leaf color change, depending on weather conditions,

as we found that these frequencies were sufficient to characterize the progression of leaf phenology in spring and fall (Klosterman et al. 2018). Images were taken at a minimum shutter speed of 1/1000 s, with constant exposure during each flight. The same ("fixed") color balance was used for all acquisition dates, because consistent color balance is necessary for reliable digital camera observations of phenology (Richardson et al. 2009). We conducted flights at mid-day (between 10 am and 3 pm) on either clear or evenly overcast days, and never during periods of variable cloud cover, as exposure was constant during flights. For each imagery acquisition date, we created orthophotos of the study area using about 100 JPEG photos taken with an intervalometer script (Canon Hack Development Kit, http://chdk.wikia.com/wiki/CHDK), with the PhotoScan photogrammetry software (Agisoft, St. Petersburg, Russia), and performed final georeferencing in ERDAS IMAGINE AutoSync (Intergraph, Huntsville, AL). The orthophotos used in this study are available through the Harvard Forest Data Archive (Klosterman and Richardson 2017b).

We calculated "start of spring" and "end of spring" phenology dates using G_{CC} and R_{CC} (defined similarly to G_{CC}) values for ROIs consisting of grid cells from a 10 m resolution grid over the aerial images. A sigmoid curve with a linear decrease in summer time greenness was used to fit G_{CC} time series, and phenology dates were estimated using extrema in the curvature change rate (Klosterman et al. 2014). For a small number of grid cells with leaves that appeared red in spring time (6 grid cells, red spring leaves only observed in 2015), we used 10 and 90% amplitude of linear interpolations of R_{CC} to calculate start and end of spring (Klosterman and Richardson 2017a). We limited our analysis to upland forest, excluding wetlands to the north and south of the study area. We then calculated average start of spring dates, and lengths of green-up (time from start to end of spring) for each grid cell of deciduous land cover for the years 2013–2015 and examined their association with linear regression.

Phenology modeling

We sought to determine whether variability in the duration of green-up could be explained by interannual temperature variation. To do this, we used a growing degree-day (GDD) model:

$$GDD_i = \sum_{t_0}^{t_{pheno}} max(0, T_i - T_b) \quad (2)$$

where t_0 is the starting date of degree-day accumulation (day of year or DOY), T_i is the daily average temperature (°C), and T_b is the base temperature above which accumulation occurs. The phenology event occurs on day t_{pheno}, when the GDD sum is greater than or equal to the critical sum F^* (°Cd).

Predictive models of budburst and leaf expansion

A model that can be used prognostically must predict budburst as well as L75. Therefore, we formulated a two-stage model (Eqs. 3 and 4) that sequentially uses Eq. 2 to predict the timing of budburst and L75. We estimated parameters for two versions of this model. In the first version, both the BB and L75 models share a common base temperature (T_b), but have different critical sums (F_1^*, F_2^*). Degree days begin accumulation on a constant day of year t_0 for F_1^*, and on the day of budburst for F_2^*. This is referred to as the one-base temperature model:

$$F_1^* = \sum_{t_i=t_0}^{t_{BB}} max(0, T_i - T_b) \quad (3)$$

and

$$F_2^* = \sum_{t_i=t_{BB}}^{t_{L75}} max(0, T_i - T_b) \quad (4)$$

In the second version, we fit separate base temperatures for two degree-day sums ($T_{b,1}$, $T_{b,2}$), the first accumulating temperatures toward budburst, and the second accumulating between budburst and L75. We did this to see whether a model allowing for different temperature responses of budburst and leaf expansion would better describe observed data than a model with a single base temperature. This is referred to as the two-base temperature model.

Model parameterization

We fit both models described in the "Predictive models of budburst and leaf expansion" section for each of the six species listed in the "In situ observations" section, using simulated annealing in Matlab. We estimated t_0, T_b, and F^* by minimizing the total residual sum of squares (RSS) across predicted BB and L75 dates. We then compared model goodness of fit using the small-sample corrected Akaike information criteria (AICc):

$$AICc = 2k + n\ln(RSS) + \frac{2k(k+1)}{n-k-1} \quad (5)$$

where k is the number of fitted model parameters (4 for the one-base temperature model, 5 for the two-base temperature model) and n is the total number of BB and L75 observations. To ensure we found optimal parameter estimates, we ran simulated annealing using all combinations of three different initial parameter values as starting points for estimation (i.e., $3^4 = 81$ starting points for the one-base temperature model and $3^5 = 243$ starting points for the two-base temperature model). We estimated uncertainty in the model parameters

by generating 1000 parameter sets for each species where the RSS of predicted BB and L75 dates passed a chi-squared test (95% confidence), and calculating the standard deviation of each parameter (Migliavacca et al. 2012; Melaas et al. 2016). Following our observation that daily average temperatures were above 0 °C during leaf expansion for all species in all years, we limited $T_{b,2} > 0$.

Ecosystem modeling with PnET

PnET-Day, an extension of the original PnET model that can be run at a daily time step, is a forest ecosystem model that has been validated using eddy covariance measurements of carbon and water fluxes at Harvard Forest, and has subroutines for ecosystem functions including photosynthesis, respiration, and evapotranspiration, as well as phenology (Aber and Federer 1992; Aber et al. 1996). The phenology sub-model for temperate deciduous trees in PnET has the same structure as the "one-base temperature" model described here, with default parameters $t_0 = 1$ (i.e., January 1), $T_b = 0$ °C, $F_1{}^* = 100$ °Cd, and $F_2{}^* = 800$ °Cd for deciduous trees (in PnET references, $F_2{}^* = 900$ °Cd since it is reported relative to January 1, as opposed to the date of budburst as formulated here). Leaf growth in PnET-Day begins on the predicted day of budburst ($F_1{}^* = 100$ °Cd) and proceeds proportionally to the fractional progress of accumulated degree days toward leaf maturity ($F_2{}^* = 900$ °Cd). Mathematically, at time step i after budburst, forest LAI (leaf area index) in the original PnET-Day model is calculated as:

$$LAI_i = \min\left(\frac{GDD_i - F_1^*}{F_2^*}, 1\right) * LAI_{max} \quad (6)$$

where LAI_{max} is the maximum growing season LAI. We evaluated the default parameterization of the PnET-Day phenology model, as well as our fitted phenology model, against observational data for red oak, the dominant deciduous tree species at Harvard Forest.

We then examined the effect of using the default PnET parameterization as well as fitted model parameters on ecosystem function, by implementing our model in PnET. We ran PnET retrospectively over the same time period used for model fitting (1993–2014). As a reference for the results of fitted and default phenology sub-models in PnET, we formulated prescribed phenology using the dates of BB and L75 for red oak. We assumed daily leaf growth proceeded in proportion to the amount of accumulated degree days as a fraction of the degree day sum on the date of L75. We used 0 °C as the base temperature for prescribed leaf growth since 1 °C was the minimum temperature during leaf out in any year. For each PnET run, we calculated the yearly average springtime (April–May–June) net primary productivity (NPP).

2.4.5 Climatic data

We used climatic data from the EMS tower at Harvard Forest (Munger et al. 2017) as drivers for phenology and ecosystem modeling based at Harvard Forest, including daily mean (average of minimum and maximum) temperature and daily photosynthetically active radiation.

Results

Later start of green-up coincides with faster green-up

We find that later start of spring correlates with faster green-up between years at the ecosystem level, within phenocam sites, using interannual anomalies from the site means (Fig. 2). The regression slope indicates − 0.47 (± 0.04 SE) days difference in green-up (i.e., shorter green-up) for every day later start of spring ($r = -0.60$, $p < 0.001$ versus a null hypothesis of zero slope, RMSE 4.2 days). The large geographic distribution of phenocam sites indicates that the relationship between start of spring and length of green-up is widespread in deciduous tree ecosystems throughout North America (site locations listed in Table S1, map in Fig. 1).

In the observations of individual trees at Harvard Forest, there was considerable variation in start and length of green-up over the study period. For the most prevalent species by basal area, red oak, BB varied from day of year 114 at the earliest to 136 at the latest, with an average of day of year 126 (May 6) while the length of green-up varied from 16 to 33 days and averaged 22 days. We find similar, although generally less significant correlations between the timing of budburst and

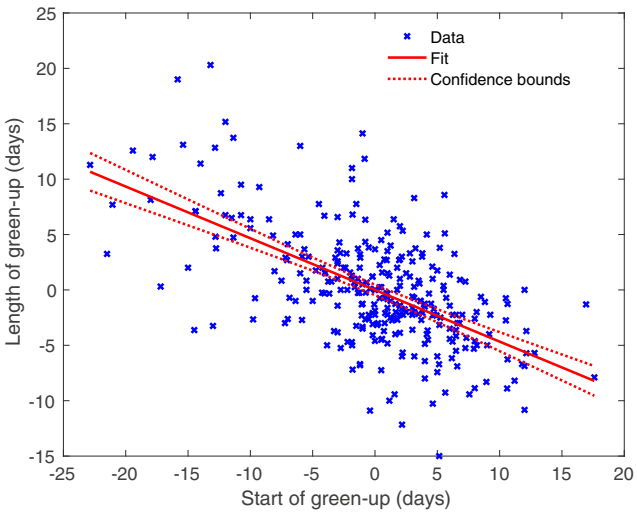

Fig. 2 Relation between length of green-up and timing of start of green-up, shown as interannual anomalies from the site mean. Negative anomalies indicate earlier start of green-up or shorter length of green-up. Three hundred one site-years from 51 PhenoCam sites having deciduous trees are shown

length of green-up for individual species at Harvard Forest (Fig. 3, Table 1), compared with the multi-site phenocam results. This is likely due in part to the sample size of individual species ($n = 22$ years), which is much smaller than the phenocam data set of interannual anomalies across sites ($n = 301$ site-years), and possibly differences in data collection method (digital image analysis versus direct observation).

Three out of six species have significant regressions with $p < 0.05$ while two of the remaining three are marginally significant at $p < 0.1$. We note that when combining all species from Harvard Forest as anomalies from the species-level means ($n = 176$ species-years), the regression is highly significant with $p < 0.001$ and a slope of -0.31 ± 0.06. This slope is lower in magnitude than what was observed across phenocam sites, although the slope for red oak, the dominant canopy deciduous species at Harvard Forest, is -0.40 ± 0.16, closer to the phenocam regression slope.

In addition to evidence for quicker progression of later springs across years for trees under direct observation, and from the integrated ecosystem-scale measurements of phenocams, we find a similar phenomenon across space within a forested ecosystem. Multi-year averages (2013–2015) of start of spring and length of green-up for 10 m grid cells of aerial drone imagery (Fig. 4) indicate that across fine-scale landscape units, there is a -1.61 ± 0.08 days change in length of green-up for every day later start of green-up ($r = -0.87$, $p < 0.001$, Fig. 4b). We note that within individual years, the correlation was significant as well ($p < 0.001$). The regression slope for the spatial relationship seen in drone imagery is steeper than the slopes for interannual relationships from phenocams and in situ observations, suggesting there is a strong link between the timing of these phenophases spatially across landscapes.

Phenology modeling and predicting ecosystem function

Following our observation in the "Later start of green-up coincides with faster green-up" section that the length of green-up is correlated with the timing of budburst, we explored how well a degree-day model could account for year to year variation in the timing of the start and end of green-up. We formulated two models. The first assumes both budburst and leaf maturity have the same base temperature for the calculation of degree days (Eqs. 3 and 4) while the second allows for different base temperatures for each process ($T_{b,1}$ for degree days prior to budburst and $T_{b,2}$ for degree days between budburst and leaf maturity). The one-base temperature model has the same structure as the phenology sub-model of PnET-Day. While the PnET-Day default parameterization sets $t_0 = 1$ (i.e., January 1), $T_b = 0$ °C, $F_1^* = 100$ °Cd, and $F_2^* = 800$ °Cd, here we optimized parameters for both the one- and two-base temperature models using phenology observations of different species from Harvard Forest. We find that both the one- and two-base temperature models had similar RMSE for most species (Table 1). Consequently, the one-base temperature model, with one less parameter, had lower AICc than the two-base temperature model for all species except yellow birch (lower AICc indicates a model is better supported by the data). Estimated parameters for the one-base temperature model indicate that the starting date of degree-day accumulation is over 2 months later than the PnET default of January 1 (range DOY 74–106 across species, standard errors ~ 1 day) and that except for yellow birch, base temperatures are greater than zero. Compared to the regression models, which predicted the length of green-up using only the timing of budburst (average model RMSE 3.7 days across species), GDD models

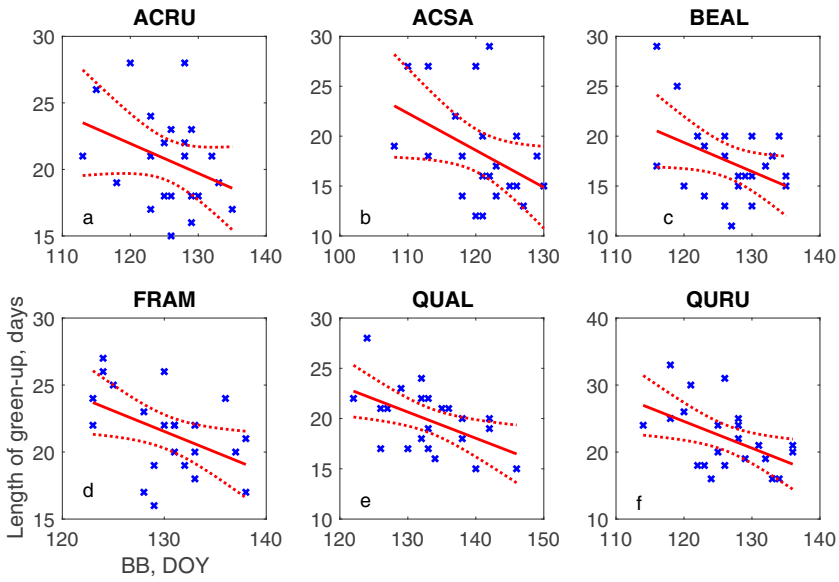

Fig. 3 Relations between the annual average timing of budburst and length of green-up for 6 species (species codes use the first two letters of the species and genus, listed in Table 1) under long-term observation at Harvard Forest (22 years of observation for each species). Data are shown as "x" symbols, regressions as solid lines, and confidence bounds as dotted lines; regression statistics shown in Table 1. There is a duplicate point for FRAM at $X = 131$, $Y = 22$

Table 1 Regression statistics (slope ± 1 SE, correlation, *p* value and RMSE) for Fig. 3. Model fitting results for the one- and two-base temperature models based on situ phenology observations from Harvard Forest, including fitted parameters ± 1 SE, and RMSEs for prediction of BB and L75 dates and length of green-up (days from BB to L75). Species are ACRU (*Acer rubrum*, red maple), ACSA (*Acer saccharum,* sugar maple), BEAL (*Betula alleghaniensis*, yellow birch), FRAM (*Fraxinus americana*, white ash), QUAL (*Quercus alba*, white oak), and QURU (*Quercus rubra*, red oak). ΔAICc indicates the difference in AICc between the two- and one-base temperature models; a positive value indicates the two-base temperature model has a larger AICc and is less supported by the data

		ACRU	ACSA	BEAL	FRAM	QUAL	QURU
Regression	Slope (dd^{-1})	− 0.22 ± 0.14	− 0.37 ± 0.18	− 0.29 ± 0.14	− 0.31 ± 0.13	0.26 ± 0.01	− 0.40 ± 0.16
	r	− 0.34	− 0.42	− 0.41	− 0.46	− 0.51	− 0.49
	p	0.122	0.051	0.057	0.031	0.014	0.020
	RMSE green-up (d)	3.5	4.8	3.8	2.8	2.8	4.3
One base temp	t_0 (DOY)	79 ± 0.74	80 ± 1.2	74 ± 1.3	106 ± 0.64	82 ± 0.70	89 ± 0.64
	T_b (°C)	1.4 ± 0.25	4.1 ± 0.41	− 4.2 ± 0.68	3.2 ± 0.45	5.8 ± 0.15	3.8 ± 0.38
	F_1* (°Cd)	264 ± 9.8	133 ± 10	549 ± 37	165 ± 12	166 ± 5.1	169 ± 12
	F_2* (°Cd)	225 ± 7.5	137 ± 8.3	288 ± 17	227 ± 9.2	152 ± 5.5	193 ± 9.0
	RMSE BB (d)	2.7	2.4	4.1	2.5	2.8	3.4
	RMSE L75 (d)	3.1	3.3	3.4	2.0	1.7	2.3
	RMSE green-up (d)	2.9	2.6	3.8	2.8	2.8	4.0
Two base temps	t_0 (DOY)	79 ± 0.68	81 ± 1.2	56 ± 1.1	106 ± 0.70	82 ± 1.2	90 ± 0.60
	$T_{b,1}$ (°C)	1.3 ± 0.21	4.7 ± 0.51	− 9.7 ± 0.66	2.6 ± 0.65	5.8 ± 0.18	3.3 ± 0.33
	$T_{b,2}$ (°C)	2.3 ± 0.75	5.3 ± 0.48	4.8 ± 0.86	1.6 ± 1.7	5.4 ± 0.72	3.8 ± 0.60
	F_1* (°Cd)	267 ± 8.3	122 ± 13	985 ± 46	180 ± 17	167 ± 6.0	175 ± 10
	F_2* (°Cd)	207 ± 16	115 ± 8.7	134 ± 15	261 ± 38	168 ± 15	201 ± 13
	RMSE BB (d)	2.7	2.5	4.1	2.5	2.8	3.5
	RMSE L75 (d)	3.1	3.2	2.9	1.9	1.8	2.2
	RMSE green-up (d)	2.9	2.8	4.0	2.7	2.3	3.7
ΔAICc		1.6	2.1	−2.4	2.7	3.4	1.5

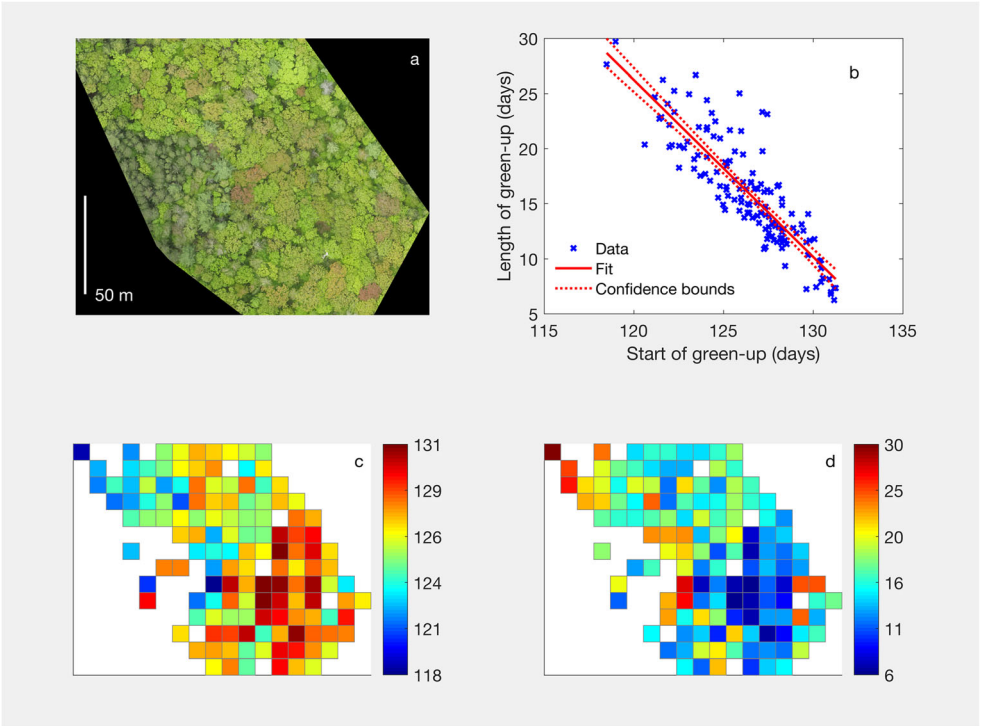

Fig. 4 **a** Aerial image of the study area at Harvard Forest in May, 2015. **b** Relation between grid cell mean start of green-up and length of green-up, for 10 m grid cells in drone imagery averaged over the years 2013, 2014, and 2015 ($n = 137$, $r = -0.87$, $p < 0.001$, slope = − 1.61 ± 0.08). **c** Start of green-up dates (day of year) for 10 m grid cells. **d** Length of green-up (days). Grid cells shown in white failed to generate dates, primarily due to low G_{CC} amplitude associated with evergreen trees

driven by temperature resulted in a better fit to the data for the duration of leaf expansion (average RMSE 3.2 days for the one-base temperature model).

Accurate representation of vegetation phenology has substantial impacts on the prediction of ecosystem services (Richardson et al. 2012). To examine the impact of the relation between the timing of budburst and velocity of green-up on NPP, we used the ecosystem model PnET driven by local climate data and phenology observations at Harvard Forest. We find that later budburst of red oak, which tended to be associated with shorter green-up (Fig. 3f), was also correlated with lower modeled spring NPP (4.5 ± 1.1 gC m^{-2} lower spring time NPP per 1 day later BB; $r = -0.69$, $p < 0.001$; Fig. S1). The latest red oak green-up of the observation period (DOY 136) was associated with a spring time NPP of as little as 203 gCm^{-2} in 1 year, while the earliest green-up (DOY 114) had an NPP of 366 gC m^{-2}, an 80% increase. These results underscore other researchers' empirical findings that the timing of spring phenophases have a large effect on early season productivity (Keenan et al. 2014).

To inform future efforts in predictive modeling of spring phenophases and their relation to ecosystem function, we compared a fitted phenology sub-model, as well as the default phenology model parameterization in PnET, to results driven by observational data. Compared to the default model, the fitted model predicted the timing of red oak BB and L75 more accurately. The tendency of the default model was to predict budburst much earlier than observed (biased 39 days early on average across years, interannual $r = 0.16$, $p > 0.05$), and L75 later than observed (biased 13 days late, $r = 0.62$, $p < 0.01$), however the fitted model had relatively little bias and relatively high interannual correlation (BB bias 1 day date, $r = 0.83$, $p < 0.001$; L75 bias 0 days, $r = 0.90$, $p < 0.001$) (Fig. 5a, b). Consequently, RMSE from the default parameters was 40 and 14 days for BB and L75, but 3.4 and 2.3 days for the fitted model, respectively.

Due to biases in modeled budburst dates, modeled NPP began to increase earlier in the year under the default model than with prescribed phenology, before reaching similar levels later in spring around DOY 140 (multi-year average NPP time series shown in Fig. 5c). Because of this, the default model resulted in an overestimate of annual spring NPP by an average of 51 gC m^{-2} per year, and overestimated total spring NPP for the 22-year period by 17% in comparison to the results from prescribed phenology (Fig. 5d). On the other hand, the fitted sub-model was within 1 gC m^{-2} per year on average and within 1% of prescribed phenology results for total spring NPP over the 22-year period. This shows that optimizing the parameters of the degree day model, as opposed to using default parameters for deciduous trees in PnET, yields results that are substantially closer to model runs driven by observational phenology data from Harvard Forest.

Discussion

We used a combination of phenological data from sources including widely geographically distributed ecosystem-scale observations (phenocams), long term observations of individual trees, and fine-scale measurements of landscape phenology with a drone to examine the association between the timing of the start of springtime canopy development and the velocity of leaf expansion. Our results show that when leaves start to develop later in the year, they proceed more quickly from budburst through leaf expansion. We noted significant interannual trends of less than 1 day faster green-up per day later start of green-up (− 0.47 ± 0.036 days per day at phenocam sites, − 0.31 ± 0.06 for trees under long-term observation). The spatial association across fine-scale landscape units within a single site was stronger (− 1.61 ± 0.08 days per day from aerial drone observations), indicating this phenomenon is both widespread and pronounced at the within-ecosystem level.

Although the phenomena of later springs greening up more quickly was not observed in a study of forest trees using 5 years of observational data (Donnelly et al. 2017), it was observed in a study of both woody and herbaceous plants from a high-Arctic site with 14 years of data (Westergaard-Nielsen et al. 2017), as well as a study comparing a canopy of forest trees in two contrasting springs (Richardson et al. 2009). In the present study, many of the phenocam sites had relatively short time series (records at 23 out of 51 sites were < 5 years). As the phenocam record grows longer, the evidence for interrelation of spring phenophases at individual sites should become clearer. Other methodologies may also provide useful tools to further examine the timing and rate of spring green-up; satellite remote sensing, such as the MODIS record (Hwang et al. 2011), would provide a landscape-level tool to integrate larger ecosystems over decadal time scales and is an interesting direction for possible future study. However we note that even phenocam records as short as 2 years allow for examination of contrasts between springs with different weather and phenology (e.g., Richardson et al. 2009), and provide a ground-truth of directly interpretable image data not available from satellite remote sensing (Klosterman et al. 2014). The large number and wide climatic distribution of phenocam sites used in this study (Fig. 1, Table S1) allowed us to leverage the power of the network in space-for-time fashion, to examine ecosystem-level correlation between the timing of the start and duration of green-up. We were able to use 301 site-years of ecosystem-scale phenocam data across multiple sites to complement 22 years of organism-scale observational data and fine-scale landscape observations (10 m resolution drone photography) from a single site. This enabled us to capture a wide range of climatic variability and spatial scale, to provide a diverse set of evidence for later springs progressing more quickly.

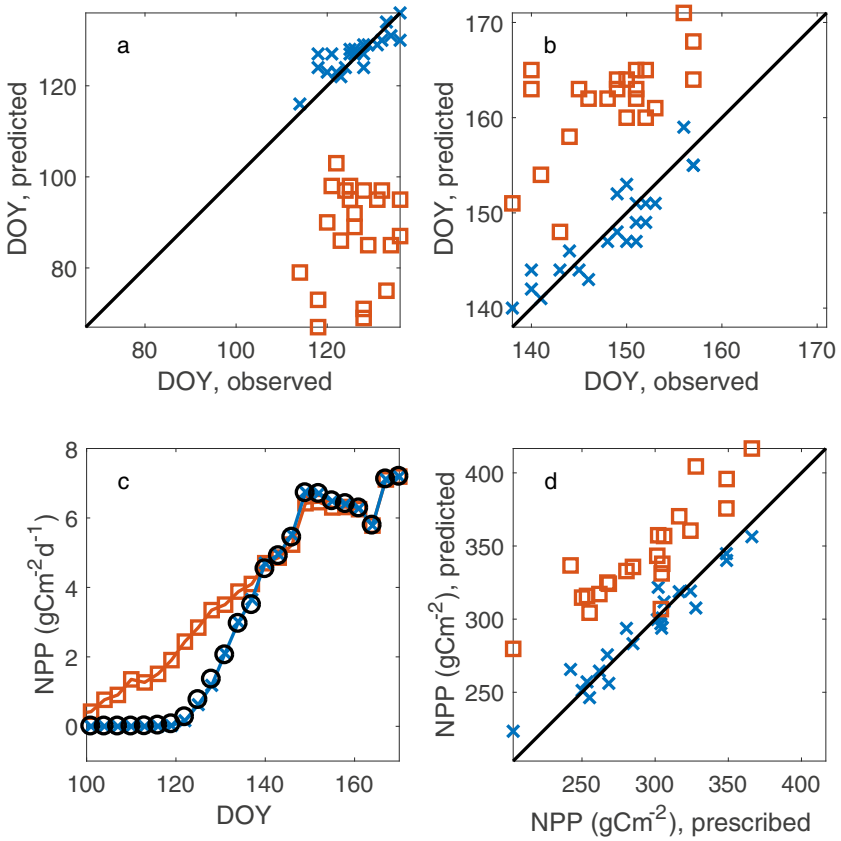

Fig. 5 **a** Predicted BB dates versus observational data for the fitted model ("x" symbols, RMSE 3.4 days, biased 1 day late on average, interannual $r = 0.83$, $p < 0.001$) and PnET default parameters (square symbols, RMSE 40 days, biased 39 days early, $r = 0.16$, $p > 0.05$). **b** The same for L75 dates (fitted model RMSE 2.3 days, biased 0 days, $r = 0.90$, $p < 0.001$; default parameters RMSE 14 days, biased 13 days late, $r = 0.62$, $p < 0.01$). **c** Three-day averaged NPP (mean across all years) during spring from prescribed runs (circle symbols), the fitted phenology model (line with "x" symbols), and the PnET default phenology parameters (line with square symbols). **d** Annual sums of modeled springtime NPP (April–May–June) for the fitted phenology model ("x" symbols) and the PnET default (square symbols), plotted against results from model runs using prescribed phenology

In examining the climatic drivers of the relationship between start and duration of leaf-out, previous research showed that over 2 years with contrasting springs, warm temperatures early in 1 year led to an earlier budburst, while subsequent cold temperatures delayed the progression of leaf expansion. However the opposite temperature phenomena in the other year led to later budburst but faster leaf development (Richardson et al. 2009). In that study, as well as others, degree-day models proved useful to represent not only the beginning, but also the duration of leaf expansion (Richardson et al. 2006; Yu et al. 2016). In this study, we parameterized-degree day models using budburst and leaf expansion data and explored whether the optimal base temperatures for budburst and leaf expansion were different. We found that for all six tree species we modeled, a single base temperature for both budburst and leaf expansion led to very similar model quality of fit (RMSEs within 1 day between the two models for each species), with the one-base temperature model better supported by the data for five species. Our results lend support to the concept of modeling leaf emergence and expansion with degree day models, although similar to what Migliavacca et al. (2012) and Richardson and O'Keefe (2009) did for budburst models, we fit all parameters of the degree day model (start date, base temperature, and critical sums) to observational data. We obtained improved results when compared with an approach using arbitrary values for parameters, such as a January 1 start date and 0 °C base temperature (Aber et al. 1996; Yu et al. 2016; Donnelly et al. 2017).

While the one-base temperature model we parameterized here has the same structure as the phenology sub-model of the ecosystem model PnET, we found that using parameters fit to observational data resulted in substantial differences in predicted springtime NPP as compared to the default parameters of PnET. The default phenology parameters resulted in NPP predictions 17% greater than PnET runs with phenology prescribed by observational data, while the fit parameters resulted in less than a 1% difference. This was mainly due to an early bias in budburst predictions relative to observations under the default parameters, similar to many terrestrial biosphere models (Richardson et al. 2012). We found that more accurate prediction of the beginning and velocity of leaf expansion improved model representation of the seasonality of NPP.

Conclusion

We found abundant evidence for a link between the timing of the start of spring and the velocity of green-up in deciduous forests of North America: when green-up starts later, it proceeds more quickly. The strongest association was noted across fine-scale landscape units within a forest ecosystem ($r = -0.87$, $p < 0.001$), although the same phenomenon was found in direct observations of trees ($p < 0.05$ for three of six species, $p < 0.1$ for two of the other three) and across 301 site-years of phenocam observations ($r = -0.60$, $p < 0.001$). We found that a degree-day model, where all the parameters had been fit using observational data, could accurately describe interannual variation in both budburst and leaf maturity using a single base temperature for both phenophase transitions. This result supports the conclusion that the faster progression of later green-ups is generally driven by the warmer temperatures that typically occur later in spring. When implemented as a subroutine of the ecosystem model PnET, the one-base temperature model fit to observational data resulted in spring NPP predictions substantially closer to results from prescribed phenology (within 1% on average over the 22-year study period), than the default phenology parameters of PnET (17% overestimate). These results illustrate the link between two key spring phenophases in deciduous forests and show the importance of accurately modeling them for predictions of ecosystem function.

Acknowledgements SK was supported by NASA Headquarters under the NASA Earth and Space Science Fellowship Program – Grant 14-EARTH14R-23. KH received support from the French National Research Agency (ANR) in the frame of the Investments for the future Programme, within the Cluster of Excellence COTE (ANR-10-LABX-45). ADR acknowledges support for the PhenoCam network from the National Science Foundation, through the Macrosystems Biology program (EF-1065029 and EF-1702697). Additional support was received from the National Science Foundation under the Harvard Forest Long-Term Ecological Research Program (DEB-1237491) and the Harvard Center for Geographic Analysis. We thank John O'Keefe of Harvard Forest for his insightful discussions of this research.

References

Aber J, Federer C (1992) A generalized, lumped-parameter model of photosynthesis, evapotranspiration and net primary production in temperate and boreal forest ecosystems. Oecologia 92:463–474

Aber JD, Reich PB, Goulden ML (1996) Extrapolating leaf CO2 exchange to the canopy: a generalized model of forest photosynthesis compared with measurements by eddy correlation. Oecologia 106: 257–265. https://doi.org/10.1007/BF00328606

Archetti M, Richardson AD, O'Keefe J, Delpierre N (2013) Predicting climate change impacts on the amount and duration of autumn colors in a new England Forest. PLoS One 8:e57373. https://doi.org/10.1371/journal.pone.0057373

Cannell M, Smith R (1983) Thermal time, chill days and prediction of budburst in Picea sitchensis. J Appl Ecol 20:951–963

Chuine I (2000) A unified model for budburst of trees. J Theor Biol 207: 337–347. https://doi.org/10.1006/jtbi.2000.2178

Donnelly A, Yu R, Caffarra A, Hanes J, Liang L, Desai AR, Liu L, Schwartz MD (2017) Interspecific and interannual variation in the duration of spring phenophases in a northern mixed forest. Agric For Meteorol 243:55–67. https://doi.org/10.1016/j.agrformet.2017.05.007

Dragoni D, Schmid HP, Wayson CA et al (2011) Evidence of increased net ecosystem productivity associated with a longer vegetated season in a deciduous forest in south-central Indiana, USA. Glob Chang Biol 17:886–897. https://doi.org/10.1111/j.1365-2486.2010.02281.x

Duveneck MJ, Thompson JR (2017) Climate change imposes phenological trade-offs on forest net primary productivity. J Geophys Res Biogeosci 122:2298–2313. https://doi.org/10.1002/2017JG004025

Fitzjarrald D, Acevedo O (2001) Climatic consequences of leaf presence in the eastern United States. J Clim 14:598–614

Gallagher JN (1979) Field studies of cereal leaf growth: I. Initiation and expansion in relation to temperature and ontogeny. J Exp Bot 30: 625–636. https://doi.org/10.1093/jxb/30.4.625

Goulden ML, Munger JW, Fan SM et al (1996) Exchange of Carbon Dioxide by a Deciduous Forest : Response to Interannual Climate Variability. Science (80) 271:1576. https://doi.org/10.1126/science.271.5255.1576

Granier C, Tardieu F (1998) Is thermal time adequate for expressing the effects of temperature on sunflower leaf development? Plant Cell Environ 21:695–703. https://doi.org/10.1046/j.1365-3040.1998.00319.x

Hunter A, Lechowicz M (1992) Predicting the timing of budburst in temperate trees. J Appl Ecol 29:597–604

Hwang T, Song C, Vose JM, Band LE (2011) Topography-mediated controls on local vegetation phenology estimated from MODIS vegetation index. Landsc Ecol 26:541–556. https://doi.org/10.1007/s10980-011-9580-8

Jeong S-J, Medvigy D, Shevliakova E, Malyshev S (2012) Uncertainties in terrestrial carbon budgets related to spring phenology. J Geophys Res 117:1–17. https://doi.org/10.1029/2011JG001868

Keenan TF, Gray J, Friedl MA, Toomey M, Bohrer G, Hollinger DY, Munger JW, O'Keefe J, Schmid HP, Wing IS, Yang B, Richardson AD (2014) Net carbon uptake has increased through warming-induced changes in temperate forest phenology. Nat Clim Chang 4:598–604. https://doi.org/10.1038/nclimate2253

Klosterman S, Richardson A (2017a) Observing spring and fall phenology in a deciduous Forest with aerial drone imagery. Sensors 17: 2852. https://doi.org/10.3390/s17122852

Klosterman S, Richardson AD (2017b) Landscape phenology from unmanned aerial vehicle photography at Harvard Forest since 2013. Harvard Forest data archive: HF294. http://harvardforest.fas.harvard.edu:8080/exist/apps/datasets/showData.html?id=hf294. Accessed 1 Dec 2017

Klosterman ST, Hufkens K, Gray JM, Melaas E, Sonnentag O, Lavine I, Mitchell L, Norman R, Friedl MA, Richardson AD (2014) Evaluating remote sensing of deciduous forest phenology at multiple spatial scales using PhenoCam imagery. Biogeosciences 11: 4305–4320. https://doi.org/10.5194/bg-11-4305-2014

Klosterman S, Melaas E, Wang J et al (2018) Fine-scale perspectives on landscape phenology from unmanned aerial vehicle (UAV) photography. Agric For Meteorol 248:397–407. https://doi.org/10.1016/J.AGRFORMET.2017.10.015

Körner C (2017) A matter of tree longevity. Science 355:130–131. https://doi.org/10.1126/science.aal2449

Melaas EK, Friedl MA, Richardson AD (2016) Multiscale modeling of spring phenology across deciduous forests in the eastern United States. Glob Chang Biol 22:792–805. https://doi.org/10.1111/gcb.13122

Menzel A, Sparks TH, Estrella N et al (2006) European phenological response to climate change matches the warming pattern. Glob Chang Biol 12:1969–1976. https://doi.org/10.1111/j.1365-2486.2006.01193.x

Migliavacca M, Sonnentag O, Keenan TF, Cescatti A, O'Keefe J, Richardson AD (2012) On the uncertainty of phenological responses to climate change and its implication for terrestrial biosphere models. Biogeosci Discuss 9:879–926. https://doi.org/10.5194/bgd-9-879-2012

Munger W, Wofsy S, Barford C, Urbanski S (2017) Canopy-atmosphere exchange of carbon, water and energy at Harvard Forest EMS tower since 1991. Harvard Forest data archive: HF004. http://harvardforest.fas.harvard.edu:8080/exist/apps/datasets/showData.html?id=hf004. Accessed 10 Dec 2017

O'Keefe J (2015) Phenology of woody species at Harvard Forest since 1990. Harvard forest data archive: HF003. http://harvardforest.fas.harvard.edu:8080/exist/apps/datasets/showData.html?id=hf003. Accessed 10 Dec 2017

Peñuelas J, Rutishauser T, Filella I (2009) Phenology feedbacks on climate change. Science (80) 324:887–888. https://doi.org/10.1126/science.1173004

Pettorelli N, Pelletier F, von Hardenberg A et al (2007) Early onset of vegetation growth vs. rapid green-up: impacts on juvenile mountain ungulates. Ecology 88:381–390. https://doi.org/10.1890/06-0875

Piao S, Friedlingstein P, Ciais P et al (2007) Growing season extension and its impact on terrestrial carbon cycle in the Northern Hemisphere over the past 2 decades. Glob Biogeochem Cycles 21. https://doi.org/10.1029/2006GB002888

Piao S, Ciais P, Friedlingstein P, Peylin P, Reichstein M, Luyssaert S, Margolis H, Fang J, Barr A, Chen A, Grelle A, Hollinger DY, Laurila T, Lindroth A, Richardson AD, Vesala T (2008) Net carbon dioxide losses of northern ecosystems in response to autumn warming. Nature 451:49–52. https://doi.org/10.1038/nature06444

Plard F, Gaillard J-M, Coulson T, Hewison AJM, Delorme D, Warnant C, Bonenfant C (2014) Mismatch between birth date and vegetation phenology slows the demography of roe deer. PLoS Biol 12:e1001828. https://doi.org/10.1371/journal.pbio.1001828

Richardson AD, O'Keefe J (2009) Phenological differences between understory and Overstory. In: Noormets A (ed) Phenology of ecosystem processes. Springer, New York, pp 87–117

Richardson AD, Bailey AS, Denny EG et al (2006) Phenology of a northern hardwood forest canopy. Glob Chang Biol 12:1174–1188. https://doi.org/10.1111/j.1365-2486.2006.01164.x

Richardson AD, Braswell BH, Hollinger DY, Jenkins JP, Ollinger SV (2009) Near-surface remote sensing of spatial and temporal variation in canopy phenology. Ecol Appl 19:1417–1428. https://doi.org/10.1890/08-2022.1

Richardson AD, Anderson RS, Arain MA, Barr AG, Bohrer G, Chen G, Chen JM, Ciais P, Davis KJ, Desai AR, Dietze MC, Dragoni D, Garrity SR, Gough CM, Grant R, Hollinger DY, Margolis HA, McCaughey H, Migliavacca M, Monson RK, Munger JW, Poulter B, Raczka BM, Ricciuto DM, Sahoo AK, Schaefer K, Tian H, Vargas R, Verbeeck H, Xiao J, Xue Y (2012) Terrestrial biosphere models need better representation of vegetation phenology: results from the north American carbon program site synthesis. Glob Chang Biol 18:566–584. https://doi.org/10.1111/j.1365-2486.2011.02562.x

Richardson AD, Keenan TF, Migliavacca M, Ryu Y, Sonnentag O, Toomey M (2013) Climate change, phenology, and phenological control of vegetation feedbacks to the climate system. Agric For Meteorol 169:156–173. https://doi.org/10.1016/j.agrformet.2012.09.012

Richardson AD, Hufkens K, Milliman T, Aubrecht DM, Chen M, Gray JM, Johnston MR, Keenan TF, Klosterman ST, Kosmala M, Melaas EK, Friedl MA, Frolking S (2018) Tracking vegetation phenology across diverse north American biomes using PhenoCam imagery. Sci Data 5:180028. https://doi.org/10.1038/sdata.2018.28

Schwartz MD, Ahas R, Aasa A (2006) Onset of spring starting earlier across the northern hemisphere. Glob Chang Biol 12:343–351. https://doi.org/10.1111/j.1365-2486.2005.01097.x

Sonnentag O, Hufkens K, Teshera-Sterne C, Young AM, Friedl M, Braswell BH, Milliman T, O'Keefe J, Richardson AD (2012) Digital repeat photography for phenological research in forest ecosystems. Agric For Meteorol 152:159–177. https://doi.org/10.1016/j.agrformet.2011.09.009

Vitasse Y, Porté AJ, Kremer A, Michalet R, Delzon S (2009) Responses of canopy duration to temperature changes in four temperate tree species: relative contributions of spring and autumn leaf phenology. Oecologia 161:187–198. https://doi.org/10.1007/s00442-009-1363-4

Westergaard-Nielsen A, Lund M, Pedersen SH, Schmidt NM, Klosterman S, Abermann J, Hansen BU (2017) Transitions in high-Arctic vegetation growth patterns and ecosystem productivity tracked with automated cameras from 2000 to 2013. Ambio 46:39–52. https://doi.org/10.1007/s13280-016-0864-8

Yu R, Schwartz MD, Donnelly A, Liang L (2016) An observation-based progression modeling approach to spring and autumn deciduous tree phenology. Int J Biometeorol 60:335–349. https://doi.org/10.1007/s00484-015-1031-9